Nanoparticle-Mediated Dual Delivery of an Antioxidant and a Peptide against the L-Type Ca^{2+} Channel Enables Simultaneous Reduction of Cardiac Ischemia-Reperfusion Injury

Naviin Hardy,[†] Helena M. Viola,[†] Victoria P. A. Johnstone,[†] Tristan D. Clemons,[†] Henrietta Cserne Szappanos,[†] Ruhani Singh,[‡] Nicole M. Smith,[‡,§] K. Swaminathan Iyer,[‡] and Livia C. Hool*[,†,⊥]

[†]School of Anatomy, Physiology and Human Biology, The University of Western Australia, Crawley, Western Australia 6009, Australia, [‡]School of Chemistry and Biochemistry, The University of Western Australia, Crawley, Western Australia 6009, Australia, [§]School of Animal Biology, The University of Western Australia, Crawley, Western Australia 6009, Australia, and [⊥]Victor Chang Cardiac Research Institute, Darlinghurst, New South Wales 2000, Australia

ABSTRACT Increased reactive oxygen species (ROS) production and elevated intracellular Ca^{2+} following cardiac ischemia-reperfusion injury are key mediators of cell death and the development of cardiac hypertrophy. The L-type Ca^{2+} channel is the main route for calcium influx in cardiac myocytes. Activation of the L-type Ca^{2+} channel leads to a further increase in mitochondrial ROS production and metabolism. We have previously shown that the application of a peptide derived against the alpha-interacting domain of the L-type Ca^{2+} channel (AID) decreases myocardial injury post reperfusion. Herein, we examine the efficacy of simultaneous delivery of the AID peptide in combination with the potent antioxidants curcumin or resveratrol using multifunctional poly(glycidyl methacrylate) (PGMA) nanoparticles. We highlight that drug loading and dissolution are important parameters that have to be taken into account when designing novel combinatorial therapies following cardiac ischemia-reperfusion injury. In the case of resveratrol low loading capacity and fast release rates hinder its applicability as an effective candidate for simultaneous therapy. However, in the case of curcumin, high loading capacity and sustained release rates enable its effective simultaneous delivery in combination with the AID peptide. Simultaneous delivery of the AID peptide with curcumin allowed for effective attenuation of the L-type Ca^{2+} channel-activated increases in superoxide (assessed as changes in DHE fluorescence; Empty NP = 53.1 ± 7.6%; NP-C-AID = 7.32 ± 3.57%) and mitochondrial membrane potential (assessed as changes in JC-1 fluoresence; Empty NP = 19.8 ± 2.8%; NP-C-AID=13.05 ± 1.78%). We demonstrate in isolated rat hearts exposed to ischemia followed by reperfusion, that curcumin and the AID peptide in combination effectively reduce muscle damage, decrease oxidative stress and superoxide production in cardiac myocytes.

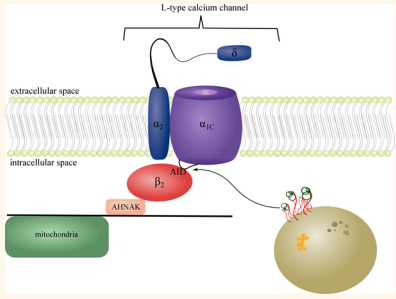

KEYWORDS: ischemia-reperfusion injury · nanoparticles · antioxidant · L-type Ca^{2+} channel · curcumin · resveratrol

Cardiovascular disease (CVD) is the leading cause of death in the western world.[1] In developed countries, ischemia-reperfusion (I-R) injury is the primary cause of morbidity and mortality associated with CVD.[2] Increases in reactive oxygen species (ROS) and intracellular Ca^{2+} are key mediators of I-R injury that contribute to the subsequent progression to cardiac hypertrophy and heart failure.[3−5] The L-type Ca^{2+} channel (LTCC) is a voltage-sensitive transmembrane protein and is the main route for Ca^{2+} influx into cardiomyocytes. The channel consists of three subunits: α_{1C}, β_{2a} and α_2-δ (Figure 1). The α_{1C} subunit is composed of four linked homologous motifs. The arrangement of these four motifs in the cell membrane forms the ion-conducting pore structure of the channel. The α_{1C} and β_{2a} subunits bind *via* the α-interacting domain (AID), located on the cytoplasmic linker connecting the first and second motifs of the α_{1C} subunit.[6] The β_{2a} subunit regulates the open probability, current amplitude and inactivation kinetics of the channel, and tethers it to actin filaments *via* the subsarcolemmal

* Address correspondence to livia.hool@uwa.edu.au.

Received for review August 13, 2014 and accepted December 10, 2014.

Published online December 10, 2014
10.1021/nn5061404

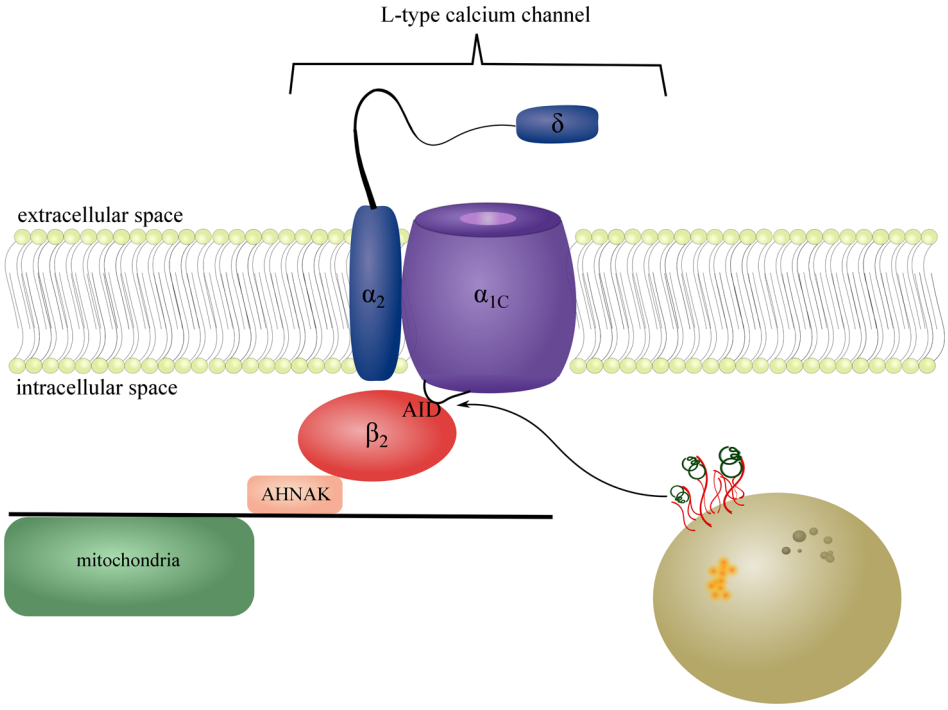

Figure 1. Schematic representation of the L-type Ca^{2+} channel (LTCC) and polymeric nanoparticles delivering antioxidant and AID peptide. LTCC, with the α-interacting domain (AID region) indicated. Polymeric nanoparticles encapsulating the antioxidant curcumin or resveratrol are shown with the AID peptide electrostatically tethered to the nanoparticle surface. AHNAK = large subsarcolemmal structural protein.

large structural protein AHNAK.[7] The LTCC has been implicated in the progression to hypertrophy following I-R injury.[8,9] It is well-known that ischemia-reperfusion results in a dramatic increase in ROS.[1] Under these conditions, the LTCC is glutathionylated and as a result undergoes conformational change that causes an increase in channel activity and Ca^{2+} conductance.[8,10] The accumulation of intracellular Ca^{2+} stimulates Ca^{2+}-dependent biochemical pathways such as the Ca^{2+} calmodulin-dependent kinases and mitogen-activated protein kinase, that lead to increased protein synthesis and development of hypertrophy.[3,11−13] The elevated intracellular Ca^{2+} levels also lead to an increase in mitochondrial Ca^{2+} uptake and mitochondrial ROS production.[8,10,14,15] The resulting increase in ROS maintains the LTCC in an active state.[8,10] This positive feedback known as "ROS-induced ROS release" plays a key role in the progression toward cardiac hypertrophy.[8,14−16] Activation of the LTCC also increases mitochondrial metabolism *via* a Ca^{2+}-independent mechanism due to the mutual attachment of the LTCC and mitochondria to the cytoskeleton.[17−19] This involves the transmission of movement of the β_{2a} subunit of the channel (after activation of LTCC) through cytoskeletal proteins to the voltage-dependent anion channel on the outer mitochondrial membrane that regulates the movement of ATP out of the mitochondria to the cytosol.[19]

We have previously reported that application of a peptide derived against the α-interacting domain of the LTCC (AID peptide) can decrease myocardial injury post reperfusion.[18,20,21] The AID peptide functionally uncouples the α_{1C} and β_{2a} subunits, disrupting cytoskeletal communication between the LTCC and the mitochondria and decreasing mitochondrial metabolic activity.[18,22,23] Application of 1 μM AID peptide reduces myocardial damage in isolated hearts following I-R injury and in rats after induction of myocardial infarction *in vivo* without causing negative inotropic effects.[20,21] This occurs as a result of a decrease in metabolic activity.[18,20,24] Effective delivery of drugs to the myocardium during reperfusion is critical to reducing the damage that leads to cardiac hypertrophy and failure. We delivered the AID peptide to the I-R injured myocardium using multifunctional polymeric nanoparticles because they represent a novel vehicle for effective delivery of drugs.[20] The nanoparticles were constructed from fluorescently labeled poly(glycidal methacrylate) (PGMA). The core encapsulated magnetite nanoparticles, rendering the system suitable for fluorescent and magnetic imaging. The high density of epoxide groups present in the PGMA core enabled covalent attachment of the cationic polymer polyethylenimine (PEI) *via* a ring opening reaction. The resulting positive surface charge was used to electrostatically tether the AID peptide to the surface. This system delivered the AID peptide more rapidly and more diffusely through the myocardium compared to conventional delivery methods using cell-penetrating peptides (CPPs), also referred to as protein transduction domains (PTDs).[20]

Elevated intracellular Ca^{2+} following I-R injury stimulates Ca^{2+}-dependent biochemical pathways. These pathways include calcineurin/nuclear factor of activated T cells, Ca^{2+} calmodulin-dependent kinases and mitogen-activated protein kinase, which also activate nuclear factor κB (NF-κB).[3,11−13] Activation of these pathways results in the mobilization of transcription factors that promote increased protein transcription and the expression of genes leading to inflammation and hypertrophy. The use of the naturally occurring antioxidants curcumin and resveratrol has been reported previously to be effective at counteracting oxidative damage and the increase in ROS accompanying I-R injury.[25] Both compounds are also potent cardioprotectants that interact with numerous biochemical pathways to mitigate I-R injury. Both compounds have been shown to reduce infarct size by up to 50%, inhibit NF-κB and prevent the development of pathological hypertrophy.[26−28] However, their efficacy has been limited by poor bioavailability, low aqueous solubility at physiological pH and difficulty in delivery to target cells.[29,30] Polymeric nanoparticles offer advantages in delivery that may overcome these obstacles.[31−33] It is widely accepted that several interdependent, concurrently occurring biochemical processes define the complexity of cardiac I-R injury. Therefore, monotherapy with a single drug that targets a single pathway may be inadequate in the treatment of I-R injury. Synergistic action using combinatorial drug treatment is an attractive strategy to prevent disease recurrence.[1] A major challenge in the development of combinatorial therapy is to unify the pharmacokinetics and cellular uptake of various therapeutics in order to allow precise control of dosage and treatment schedules. In this article we examine the efficacy of simultaneous delivery of the AID peptide in combination with antioxidants curcumin or resveratrol using multifunctional PGMA nanoparticles on myocardial damage and oxidative stress following I-R injury in isolated rat hearts

RESULTS AND DISCUSSION

Nanoparticle Characterization and Therapeutic Loading. The multifunctional PGMA nanoparticles utilized in this study were prepared from an oil in water emulsion process which yielded nanoparticles that had a z-averaged hydrodynamic diameter of 152 nm (95% confidence interval 75−335 nm; PDI: 0.062) for the curcumin loaded nanoparticles and 129 nm (95% confidence interval 58−335 nm; PDI: 0.097) for the resveratrol loaded nanoparticles following PEI attachment (see Figure S1 in Supporting Information for nanoparticle characterization). Antioxidant loading within the nanoparticles was determined by HPLC. We found that encapsulation of curcumin and resveratrol in the PGMA nanoparticle constructs differed. The loading efficiency of curcumin was 11.8% (w/w), compared to 1.0% (w/w) for resveratrol. Loading of the therapeutic AID peptide was achieved through electrostatic attraction between the highly cationic PEI chains on the surface of the nanoparticles and the negatively charged peptide as has been described previously.[20] Through this method the average loading efficiency of the therapeutic AID peptide on the nanoparticles was 12.5% w/w. The release kinetics of both resveratrol and curcumin were monitored *in vitro* (see Figure S2, Figure S3 and Methods for details). The resveratrol nanoparticles with lower loading had a fast release profile when compared to the curcumin nanoparticles, which had high loading and a slower sustained release profile over the 60 min reperfusion/therapy window.

Efficacy of Nanoparticle Delivery at Reducing I-R Injury in Isolated Hearts. We investigated the effect of nanoparticle delivery of curcumin and resveratrol in the presence or absence of the AID peptide on myocardial damage in response to I-R injury *ex vivo* in rat hearts by measuring creatine kinase (CK) and lactate dehydrogenase (LDH) release into cardiac perfusate. We have found previously that 10 μM AID is effective at decreasing myocardial injury and increasing GSH/GSSG ratio post I-R.[24] We tethered 1 μM AID peptide to NP's because this concentration is effective at decreasing CK and LDH without significantly increasing GSH/GSSG ratio.[18,20,24] This allowed us to assess an additive effect of the antioxidants. Hearts were perfused retrogradely with Ca^{2+}-containing KHB solution for 30 min, followed by 50 min global no flow ischemia then 60 min reperfusion. Nanoparticle treatments were administered at the time of reperfusion. These included either empty nanoparticles (NP), curcumin loaded (NP-C), AID peptide tethered nanoparticles containing curcumin (NP-C-AID), resveratrol loaded nanoparticles (NP-R), AID peptide tethered nanoparticles containing resveratrol (NP-R-AID) or AID peptide tethered nanoparticles (NP-AID).

Consistent with previous studies, exposure of hearts to empty nanoparticles (NP) resulted in a significant increase in CK and LDH release in response to I-R injury (Figure 2A-D).[20] Consistent with an increase in oxidative stress after application of NP's during reperfusion, the GSH/GSSG ratio was decreased (Figure 2E). Exposure of hearts to NP-AID, NP-C or NP-C-AID resulted in a significant reduction in CK and LDH release at 15, 30, 45, and 60 min following reperfusion compared to NP ($p < 0.05$, ANOVA) (Figure 2A and C). However, only NP-C and NP-C-AID decreased oxidative stress in the tissue because GSH/GSSG ratio was increased (Figure 2E). Exposure of hearts to NP-R-AID resulted in significant reduction in CK and LDH release at 15, 30, 45, and 60 min following reperfusion compared to NP (Figure 2B and D). However, application of NP-R reduced CK and LDH release at 15 and 30 min but appeared to increase at 45 and 60 min post reperfusion (Figure 2B and D) suggesting that myocardial injury was occurring but release of CK and LDH was delayed.

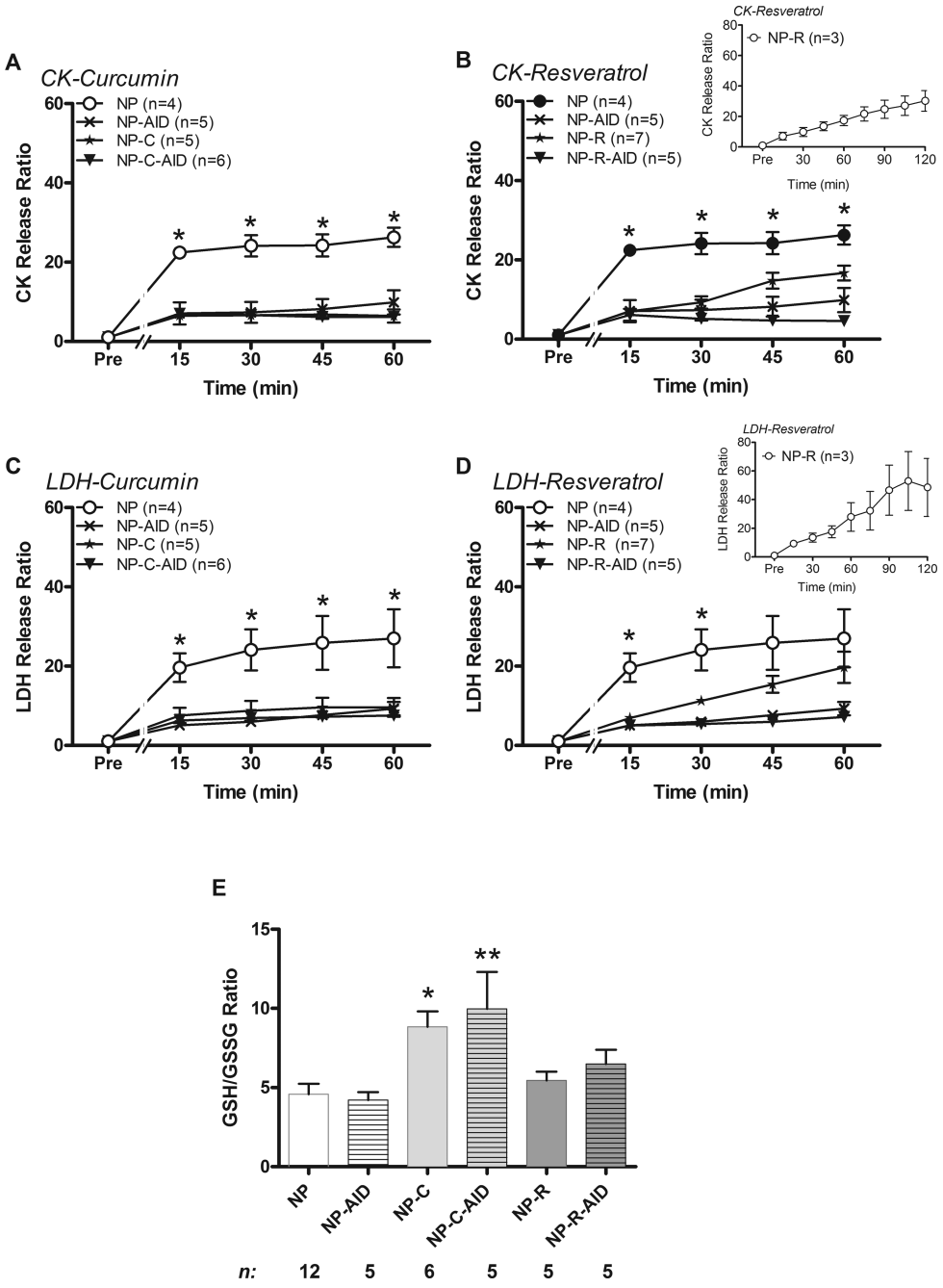

Figure 2. Effect of nanoparticles on muscle damage and oxidative stress in isolated rat hearts. (A–D) Creatine kinase (CK) and lactate dehydrogenase (LDH) release measured in perfusate samples following 50 min of global no flow ischemia. Perfusate samples were collected during 60 min of reperfusion with empty nanoparticles (NP), curcumin (NP-C) or resveratrol (NP-R) containing nanoparticles and AID peptide nanoparticles that were empty (NP-AID), contained curcumin (NP-C-AID) or contained resveratrol (NP-R-AID) as indicated and normalized to the CK or LDH released prior to the commencement of ischemia (Pre). Inset at right: CK and LDH release up to 120 min after reperfusion in the presence of NP-R as indicated. (E) GSH/GSSG ratio in homogenized cardiac tissue after 60 min of reperfusion with nanoparticles as indicated. n: represents the number of hearts. * represents $P < 0.05$ and ** represents $P < 0.01$ compared to NP.

In addition we recorded a low GSH/GSSG ratio at 60 min after application of NP-R indicating the tissue remained oxidized (Figure 2E). To further confirm that release of CK and LDH was delayed we measured CK and LDH release up to 120 min after application of NP-R post reperfusion. Consistent with continued myocardial injury, CK and LDH increased after 45 min and continued to increase up to 120 min after application of NP-R (inset at right Figure 2B and inset at right Figure 2D). These data suggest that low loading and fast release of resveratrol from PGMA nanoparticles negates its efficacy to be used as a combinatorial platform at reducing myocardial injury or oxidative stress post ischemia-reperfusion

Effect of Nanoparticle Delivery on Superoxide Production. We measured the effect of nanoparticle delivery of curcumin and resveratrol in the presence or absence

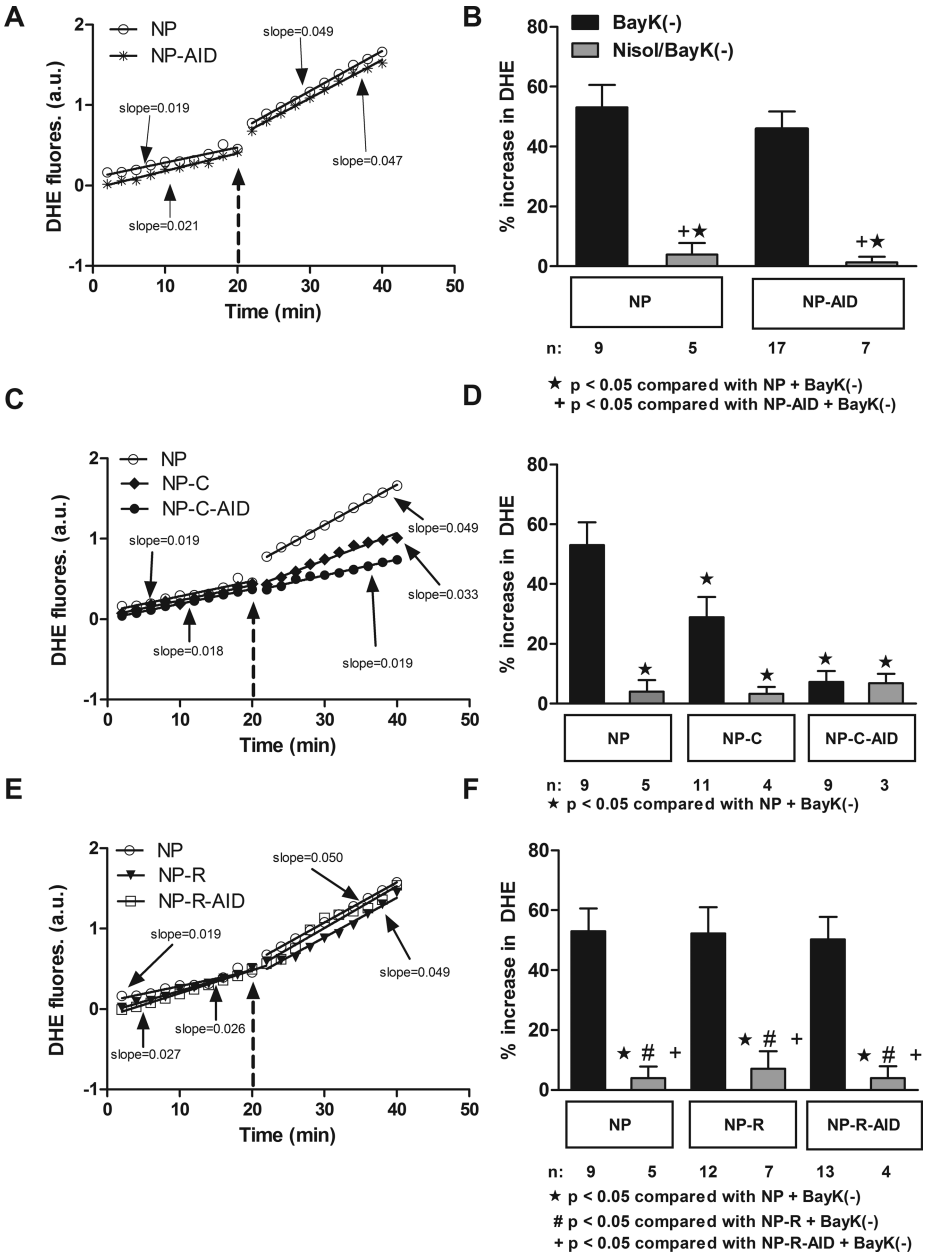

Figure 3. Curcumin and AID tethered nanoparticles significantly attenuate cellular superoxide *in vitro*. (A) DHE fluorescence (DHE fluores.) recorded from myocytes before and after addition of 10 μM BayK(−) following preincubation with NP or AID peptide nanoparticles (NP-AID). The arrow indicates where BayK(−) was added. (B) Mean ± SEM of the ratio of the rise in DHE fluorescence for myocytes exposed to NP or NP-AID as indicated. (C) DHE fluorescence (DHE fluores.) recorded from myocytes before and after addition of 10 μM BayK(−) following preincubation with NP or curcumin nanoparticles with (NP-C-AID) or without (NP-C) the AID peptide. The arrow indicates where BayK(−) was added. (D) Mean ± SEM of the ratio of DHE fluorescence for myocytes exposed to NP, NP-C or NP-C-AID as indicated. (E) DHE fluorescence (DHE fluores.) recorded from myocytes before and after addition of 10 μM BayK(−) following preincubation with NP or resveratrol nanoparticles with (NP-R-AID) or without (NP-R) the AID peptide. The arrow indicates where BayK(−) was added. (F) Mean ± SEM of the ratio of DHE fluorescence for myocytes exposed to NP, NP-R or NP-R-AID as indicated. * represents $P < 0.05$ compared to NP + BayK(−), # represents $P < 0.05$ compared to NP-R + BayK(−) and + represents $P < 0.05$ compared to NP-R-AID + BayK(−). *n* = number of cells; a.u. = arbitratry units.

of the AID peptide on superoxide in isolated mouse cardiac myocytes using the fluorescent indicator dihydroethidium (DHE). Myocytes were preincubated with nanoparticle treatments for 20 min prior to experimentation. Consistent with previous studies, exposure of myocytes to BayK(−), an LTCC agonist, resulted in a 53.1 ± 7.6% increase in DHE signal in the presence of empty nanoparticles (NP, Figure 3A and B). The response was attenuated by the LTCC antagonist nisoldipine. Exposure of myocytes to NP-AID or NP-C resulted in a partial but significant decrease in DHE signal in response to BayK(−) compared to NP (Figures 3A−D). Exposure of cardiac myocytes to NP-C-AID caused a significantly greater decrease in

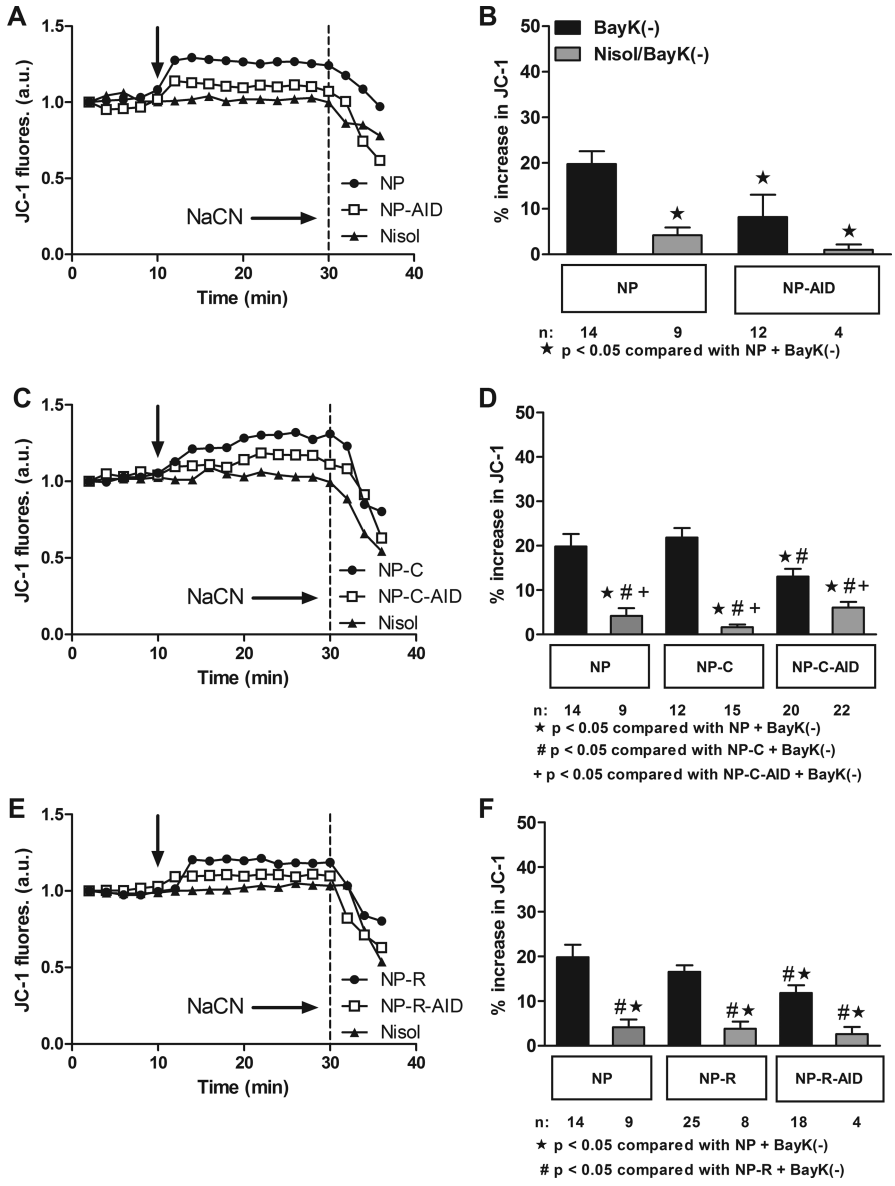

Figure 4. Curcumin and resveratrol loaded nanoparticles have no effect on ψ_m *in vitro*. (A) Representative traces of JC-1 fluorescence recorded in individual myocytes before and after exposure to 10 μM BayK(−) after incubation with NP, AID peptide-tethered nanoparticles (NP-AID) or nisoldipine (Nisol). The arrow indicates where BayK(−) was added. 4 mM sodium cyanide (NaCN) was added to collapse ψ_m. (B) Mean ± SEM of changes in ratiometric JC-1 fluorescence for myocytes exposed to NP or NP-AID as indicated. (C) Representative traces of JC-1 fluorescence recorded in myocytes before and after exposure to 10 μM BayK(−), following treatment with NP, curcumin nanoparticles with (NP-C-AID) or without (NP-C) the AID peptide or nisoldipine (Nisol). The arrow indicates where BayK(−) was added. 4 mM sodium cyanide (NaCN) was added to collapse ψ_m. (D) Mean ± SEM of changes in ratiometric JC-1 fluorescence for myocytes exposed to NP, NP-C or NP-C-AID as indicated. (E) Representative traces of JC-1 fluorescence recorded in myocytes before and after exposure to 10 μM BayK(−), following a preincubation with NP, resveratrol nanoparticles with (NP-R-AID) or without (NP-R) the AID peptide or nisoldipine (Nisol). The arrow indicates where BayK(−) was added. 4 mM sodium cyanide (NaCN) was added to collapse ψ_m. (F) Mean ± SEM of changes in ratiometric JC-1 fluorescence for myocytes exposed to NP, NP-R or NP-R-AID as indicated. * represents $P < 0.05$ compared to NP + BayK(−), # represents $P < 0.05$ compared to NP-C + BayK(−) and + represents $P < 0.05$ compared to NP-C-AID + BayK(−). n = number of cells; a.u. = arbitratry units.

DHE signal in response to BayK(−) compared to NP (Figures 3C and D). However, exposure of cardiac myocytes to NP-R or NP-R-AID did not significantly alter DHE signal in response to BayK(−) (Figure 3E and F). These data provide evidence that NP-C-AID may be most effective in reducing oxidative stress in response to activation of the LTCC compared to NP-C, NP-R or NP-R-AID. Elevated ROS production is a key mediator in the development of myocardial injury following ischemia-reperfusion.[34] Attenuating the increase in ROS following I-R is critical to reducing the development of myocardial injury. Production of ROS peaks early following reperfusion,[35] causing covalent modification of the LTCC.[10] The effects of a short exposure to excess ROS persist for many hours.[8] Mitigating the increase in ROS is important to reduce myocardial damage caused by oxygen radicals. The ability of nanoparticle-assisted delivery of curcumin to attenuate both muscle damage

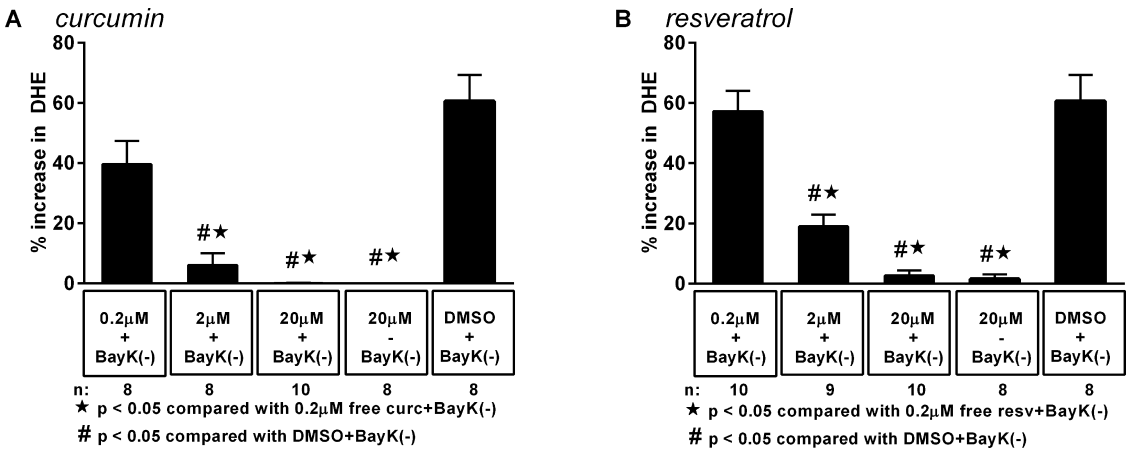

Figure 5. Concentration-dependent inhibition of DHE signal by curcumin and resveratrol in the absence of nanoparticles. (A) Mean ± SEM of the ratio of the BayK(−)-stimulated increase in DHE fluorescence for myocytes preincubated for 20 min with curcumin at 0.2, 2, 20 μM or DMSO only. (B) Mean ± SEM of the ratio of the BayK(−)-stimulated increase in DHE fluorescence for myocytes preincubated for 20 min with resveratrol at 0.2, 2, 20 μM or DMSO only, as indicated. * represents $P < 0.05$ compared to 0.2 μM free curcumin or resveratrol as indicated and # represents $P < 0.05$ compared to DMSO+BayK(−). n = number of cells. The lack of bar graph indicates complete attenuation of BayK(−)-stimulated increase in DHE signal by curcumin or no change in basal DHE signal by curcumin in the absence of BayK(−) as indicated.

and oxidative stress simultaneously in isolated hearts suggests this may be an effective treatment following I-R injury.

Effect of Nanoparticle Delivery on Mitochondrial Membrane Potential. Activation of the LTCC has been shown to increase mitochondrial metabolism *via* a Ca^{2+}-independent mechanism due to mutual attachment of the LTCC and mitochondria to the cytoskeleton.[17−19,24] This is assessed as changes in mitochondrial membrane potential (ψ_m) in cardiac myocytes. Application of 1 μM AID peptide can partially attenuate the increase in ψ_m in cardiac myocytes after activation of LTCC.[20,24] We examined the effect of nanoparticle delivery of curcumin and resveratrol in the presence or absence of the AID peptide on ψ_m in isolated mouse cardiac myocytes using the fluorescent indicator JC-1. Myocytes were preincubated with nanoparticle treatments for 20 min prior to experimentation. Consistent with previous studies, exposure of myocytes to BayK(−) resulted in a 19.8 ± 2.8% increase in JC-1 signal in the presence of empty nanoparticles (NP, Figure 4).[17] The response was attenuated by nisoldipine. Exposure of myocytes to NP-AID significantly reduced the BayK(−) stimulated increase in JC-1 signal compared to NP ($p < 0.05$, ANOVA) (Figure 4A and B). Exposure of myocytes to NP-C-AID but not NP-C resulted in a significant reduction in JC-1 signal in response to BayK(−) (Figure 4C and D). Similarly, exposure of myocytes to NP-R-AID but not NP-R caused a significant reduction in JC-1 signal in response to BayK(−) (Figure 4E and F). Application of sodium cyanide (NaCN) at the end of each experiment verified the JC-1 signal was mitochondrial in origin. These data confirm that the AID peptide can significantly attenuate BayK(−) induced increases in ψ_m. These data are consistent with the proposed mechanism of action of the AID peptide, which functionally uncouples the α_{1C} and β_{2a} subunits of the LTCC.[23] The uncoupling disrupts the interaction between the LTCC and the cytoskeleton, preventing changes in mitochondrial membrane potential and metabolism in response to activation of the channel.[7,18]

Antioxidant Capacity of Curcumin and Resveratrol. We investigated the antioxidant capacity of curcumin and resveratrol *in vitro* in the absence of nanoparticles in order to estimate effective working concentrations of antioxidant. Isolated cardiac myocytes were preincubated for 20 min with curcumin or resveratrol dissolved in DMSO at concentrations of 0.2, 2, and 20 μM. BayK(−) stimulated increases in superoxide production (as measured by DHE fluorescence) were significantly decreased by curcumin and resveratrol at 2 and 20 μM compared to 0.2 μM antioxidant and DMSO only controls (Figure 5). This confirms that curcumin and resveratrol are potent antioxidants *in vitro* at concentrations above a therapeutic threshold that lies between 0.2−2 μM. Indeed the concentrations of resveratrol and curcumin in the NP-R-AID and NP-C-AID formulations (both administered at 1 μM AID peptide concentration) were 0.82 μM (at 1 wt % loading) and 7.2 μM (at 11.8 wt % loading), respectively. On the basis of the release profiles (Figure S2 and S3) it becomes obvious that the amount of curcumin released from the nanoparticles during 60 min of reperfusion was above the therapeutic threshold window of 0.2−2 μM. The same did not hold true for resveratrol, as NP-R and NP-R-AID did not alter DHE signal. This was despite a significant effect of free resveratrol on BayK(−) stimulated increase in DHE signal (Figure 5). We propose this was a consequence of the lower encapsulation of resveratrol coupled with its fast release kinetics. Indeed the initial burst release from NP-R reduced CK and LDH release at 15 and

30 min; however, the lower loading failed to control the increase at 45 and 60 min post reperfusion.

CONCLUSION

Encapsulating curcumin in PGMA nanoparticles in the presence or absence of tethered AID peptide is an effective combination for simultaneous action in the reduction of myocardial damage and oxidative stress following ischemia-reperfusion *ex vivo* in rat hearts. Combinatorial trials involving resveratrol proved less effective, and are therefore not a viable candidate for simultaneous therapy. Nanoparticles encapsulating the antioxidant curcumin significantly decreased superoxide production in response to activation of the LTCC in isolated cardiac myocytes. The response was more potent when myocytes were treated with curcumin loaded nanoparticles that were tethered with the AID peptide. This additive effect appears to be due to a decrease in metabolic activity in the myocytes by the AID peptide. Importantly, *in vitro* analysis revealed that curcumin and the AID peptide reduce I-R injury *via* different mechanisms demonstrating that this combination would potentially be expected to be more effective than either therapeutic alone in an *in vivo* setting.

METHODS

Nanoparticle Synthesis. *Magnetite Synthesis.* Monodispersed magnetite nanoparticles were synthesized by thermal decomposition as described by Sun *et al.*[36] In brief, iron(III) acetylacetonate (2 mM), 1,2-tetradecandiol (10 mM), oleic acid (6 mM), oleylamine (6 mM) and benzyl ether (20 mL) were mixed with a magnetic stirrer and heated to 100 °C for 1 h. The mixture was heated to 200 °C under an atmosphere of N_2 for 2 h and then heated to reflux (~300 °C) for 1 h. The reaction mixture cooled overnight under an atmosphere of N_2 and was precipitated in ethanol (40 mL) and centrifuged at 3000*g* for 15 min. The precipitate was resuspended in hexane (7.5 mL) and centrifuged again under identical conditions. The supernatant containing magnetite nanoparticles was stored under argon until use.

Polymer Nanoparticle Synthesis. Nanoparticles were synthesized by an oil-in-water emulsion process as described previously, with modification.[37] Dry PGMA (100 mg) was dissolved in methyl ethyl ketone (MEK; 9 mL). Dry magnetite nanoparticles (25 mg) were dispersed in chloroform (3 mL) containing dissolved resveratrol (25 mg) or curcumin (25 mg). The two organic solvents were mixed and added dropwise to an aqueous solution of the polymer Pluronic F-108 (12.5 mg/mL, 30 mL) that was vigorously stirring to form a vortex. The resulting emulsion was ultrasonicated at low power for 1 min to form the nanoparticles. The organic phase was evaporated under low N_2 flow overnight. Excess polymer and aggregated magnetite were removed by centrifugation at 3000*g* for 45 min. The nanoparticles contained in the supernatant were collected on a magnetic separation column (LS, Miltenyi Biotec) and washed and eluted using Milli-Q water (pH 5.8).

PEI Attachment. Nanoparticles were precipitated by centrifugation at 14000*g* for 30 min and the pellet resuspended in Pluronic F-108 solution (2.5 mg/mL, 30 mL) containing polyethylenimine (PEI 50% solution M_n 1200, M_w 1300) (20 mg/mL) adjusted to pH 6.5. Nanoparticles were reacted in this solution at room temperature for 48 h to allow for PEI attachment before being reprecipitated *via* centrifugation at 14000*g* for 30 min. Unattached PEI was removed by repeated washing and centrifugation of the precipitated nanoparticles in Milli-Q water. Nanoparticles were stored as a concentrated stock at 4 °C and protected from light to prevent degradation of the light-sensitive antioxidants. The final concentration of nanoparticles was determined by lyophilization.

AID Peptide Conjugation. A peptide against the alpha-interacting domain in the I–II linker of the α_{1C} subunit was synthesized using the amino acid sequence QQLEEDLKGYLDWITQAE as previously described [23] (Auspep Pty Ltd., Parkville, Australia). PEI-attached nanoparticles (400 μL of 2 mg/mL stock) were incubated with 400 μM AID peptide (400 μL) for 1 h (empty nanoparticles), 24 h (resveratrol nanoparticles) or 48 h (curcumin nanoparticles) at room temperature. Subsequent centrifugation at 16000*g* for 30 min separated the nanoparticles and tethered AID peptide from the free peptide in solution. The supernatant was removed and the nanoparticles were resuspended in an appropriate volume of Milli-Q water to obtain a final peptide concentration of 100 μM. The AID peptide tethered nanoparticles were stored at 4 °C in glass vials for no longer than 3 weeks.

Nanoparticle Characterization. *Dynamic Light Scattering (DLS).* Polymer nanoparticles were prepared for DLS and surface charge measurements by holding the samples on a magnetic separation column and washing repeatedly with Milli-Q water. Nanoparticle size and surface charge measurements were averaged over 10 runs and each measurement was conducted in triplicate. Results are presented as mean ± standard deviation.

High Performance Liquid Chromatography. Antioxidant loading of polymer nanoparticles was determined by reverse-phase HPLC. Lyophilized nanoparticles were resuspended in methanol to obtain a final nanoparticle concentration of 1 mg/mL. The samples were ultrasonicated in a water bath for 15 min and incubated for a further 45 min at room temperature to dissolve encapsulated antioxidant. Nanoparticles were separated from the solubilized antioxidant by centrifugation at 14000*g* for 30 min. Three aliquots of the supernatant (150 μL) were analyzed on a Waters 2695 HPLC with a Waters 2489 UV/vis detector using isocratic elution through a C_{18} analytical column (150 × 4.60 mm, 5 μm, 25 ± 5 °C). A mobile phase of acetonitrile:water (1% acetic acid; adjusted to pH 3.0 using 50% triethanolamine) in the ratio 45:55 (v/v) was utilized for curcumin, as described previously.[38] The mobile phase was pumped through the column at the flow rate of 1.5 mL/min with a run time of 10 min. The injection volume was 20 μL and each aliquot was injected in triplicate with single wavelength detection at 254 nm. The area under the largest peak between the retention time 7–8 min was integrated and used to calculate the concentration of curcumin by comparison to a previously prepared standard curve (R^2 = 0.9969).

For resveratrol, the method of Ansari *et al.* was modified and a mobile phase of 0.25% (v/v) acetic acid in methanol and water (52:48 v/v) was used.[39] The mobile phase was pumped through the column at the flow rate of 1.5 mL/min with a run time of 10 min. The injection volume was 20 μL and each aliquot was injected in triplicate with single wavelength detection at 303 nm. The area of the largest peak with retention time between 3.5 and 4.5 min was used to calculate the concentration of resveratrol by comparison to a standard curve (R^2 = 0.9999).

The loading efficiency and encapsulation efficiency of antioxidant in the nanoparticles were calculated with the following formulas:

$$\text{loading efficiency (\%)} = \frac{\text{mass (antioxidant in nanoparticles)}}{\text{mass (nanoparticles)}} \times 100$$

All values are quoted as mean ± standard deviation.

UV–Vis Spectrophotometry. The binding of the AID peptide to the nanoparticles was quantified by measuring the optical absorbance of the supernatant following incubation and centrifugation at 280 nm with a UV–vis spectrophotometer (Nanodrop 1000). The concentration of AID peptide in the

supernatant was calculated by comparison to a previously prepared standard curve ($R^2 = 0.9980$). The difference between the initial concentration of the AID peptide (400 μM) and the concentration of the peptide in the supernatant was used to determine the amount attached to the nanoparticles. The absorbance in the supernatant was measured in triplicate for each of three separate aliquots.

Cardiac I-R Injury. *Langendorff I/R Heart.* Hearts of 6−8 week old male Wistar rats were excised and perfused retrogradely *via* the aorta on a Langendorff apparatus with Ca^{2+}-containing Krebs-Henseleit buffer (KHB) containing: 120 mM NaCl, 25 mM $NaHCO_3$, 4.8 mM KCl, 2.2 mM $MgSO_4$, 1.2 mM NaH_2PO_4 and 11 mM glucose as described previously.[40] Hearts were perfused for 30 min at a constant pressure of 80 cmH_2O. No-flow ischemia was induced by stopping the flow of perfusate for 50 min, followed by 60 min of reperfusion. At the onset of reperfusion, nanoparticles were delivered directly to the coronaries *via* the aorta and continued exposure was ensured *via* a recirculation system. The concentration of AID peptide tethered to nanoparticles was 1 μM. Nanoparticles without the AID peptide attached were delivered at the same nanoparticle concentration used to deliver the AID peptide. Following 60 min of reperfusion with Ca^{2+}-containing KHB, hearts were perfused for a further 10 min with Ca^{2+}-free KHB before removal from the Langendorff apparatus and storage in Ca^{2+}-free KHB on ice for assaying of reduced to oxidized glutathione. Perfusate samples (~2 mL) were collected at 20 and 25 min of perfusion and again at 0, 15, 30, 45, and 60 min of reperfusion. All perfusate samples were stored at 4 °C until used for CK and LDH assays.

Glutathione Assay. The ratio of the reduced (GSH) and oxidized (GSSG) forms of glutathione was determined according to Rahman *et al.*[41] Potassium phosphate EDTA buffer (KPE) was prepared by dissolving EDTA disodium salt in 0.1 M potassium phosphate buffer (pH 7.5). Extraction buffer (EB) was prepared by dissolving sulfosalicyclic acid and Triton X-100 in KPE buffer adjusted to pH 6.8. A 10% solution of 2-vinylpyridine and a 16.7% solution of triethanolamine were prepared in KPE buffer. A GSSG standard curve ranging from 10 to 80 μg/mL was prepared by dissolving GSSG in EB. A GSH standard curve was prepared similarly using pH 6.8 EB.

GSSG and GSH standards and samples were loaded in triplicate into a 96-well plate. DTNB and ß-NADPH were prepared in KPE buffer. Glutathione reductase (GR) reagent was prepared by diluting GR in KPE. Equal volumes of GR reagent and DTNB were mixed immediately prior to commencing the assay. GR was added to each sample and standard in the 96-well plate and incubated for 30 s before the reaction was initiated with the addition of β-NADPH. The optical absorbance was monitored at 412 nm (PowerWave XS, BioTek) at 25 °C every 8 s for 2 min. A least-squares regression line was fitted to the linear portion of the curve. The gradient of each standard was plotted against its concentration to produce a standard curve used to determine GSH and GSSG concentration in each sample. The oxidized to reduced ratio was calculated by dividing the concentration of GSH by the concentration of GSSG.

Creatine Kinase Assay. Creatine kinase (CK) activity was measured in all perfusate samples using a Randox CK-NAC diagnostic kit (Randox Laboratories) as described previously.[10] Perfusate was added to CK enzyme reagent (Randox) and the rate of increase of optical absorbance was monitored at 340 nm (PowerWave XS, BioTek) for 15 min at 30 °C. All samples were measured in triplicate. The gradient was converted to CK activity using the equation:

$$\text{CK activity (U/L)} = \frac{4127 \times (\Delta\text{Abs 340 nm})}{\text{min}}$$

The average value of CK activity in the samples collected at 20 and 25 min of perfusion (prior to ischemia) was set to 1 and used to normalize CK activity measured during reperfusion.

Lactate Dehydrogenase Assay. The activity of lactate dehydrogenase (LDH) in each perfusate sample was determined by measuring the rate of decrease in absorbance at 340 nm (PowerWave XS, BioTek) over 15 min at 25 °C as described previously.[10] Briefly, 150 μL of perfusate was mixed with 50 μL of LDH assay buffer (50 mM imidazole, 4 mM pyruvate, 0.05% BSA, 375 μM NADH, pH 7.0) and the absorbance measured immediately. All samples were measured in triplicate. The activity of LDH in the sample was calculated with the equation:

$$\text{LDH activity (U/mL)} = \frac{\left(\frac{\Delta\text{Abs 340 nm}}{\text{min}}[\text{test}] - \frac{\Delta\text{Abs 340 nm}}{\text{min}}[\text{blank}]\right)}{6.22 \times 0.15}$$

LDH activity in perfusate samples collected during reperfusion was normalized to preischemia activity (the average of 20 and 25 min of perfusion).

***In Vitro* Data.** *Isolation of Mouse Ventricular Myocytes.* Myocytes were isolated from 8-week old male C57Bl/6J mice using a collagenase dissociation method as described previously.[42] Animals were anesthetized by an intraperitoneal injection of pentabarbitone sodium (240 mg//kg) prior to excision of the heart as approved by The Animal Ethics Committee of The University of Western Australia in accordance with the *Australian Code of Practice for the Care and Use of Animals for Scientific Purposes* (NH&MRC, 8th ed., 2013). For all *in vitro* experiments, myocytes were preincubated with the nanoparticles for 20 min prior to commencing fluorescent measurements. AID peptide-tethered nanoparticles were delivered at a peptide concentration of 1 μM. All other nanoparticles were delivered at a nanoparticle concentration of 2 μg/mL.

Measurement of Mitochondrial Membrane Potential. Mitochondrial membrane potential was recorded in mouse ventricular myocytes using the fluorescent indicator 5,5′,6,6′-tetrachloro-1,1′,3,3′-tetraethylbenzimidazolylcarbocyanine iodide (JC-1, 200 nM, excitation 480 nm, emission 590/520 nm; Molecular Probes) in HEPES-buffered solution at 37 °C as previously described.[8] The fluorescent signal was measured on a Hamamatsu Orca ER digital camera attached to an inverted Nikon TE2000-U microscope. Mitochondrial membrane potential was expressed as a ratio of fluorescent emission (580 nm/520 nm) normalized to the pretreatment fluorescent baseline. Fluorescent ratios recorded over 6 min before and after treatments were averaged and alterations in fluorescent ratio were reported as percentage increase from the baseline average. JC-1 fluorescence was stimulated by the addition of the LTCC agonist BayK(−) (10 μM). The channel antagonist nisoldipine (20 μM) was used to verify increases in fluorescence were a result of BayK(−) stimulation. To verify that the JC-1 signal represented mitochondrial membrane potential, 40 mM NaCN was added at the end of each experiment to collapse mitochondrial membrane potential. Data were analyzed in Metamorph 6.3.

Measurement of Superoxide. Generation of superoxide was measured in mouse ventricular myocytes using the fluorescent indicator dihydroethidium (DHE 5 μM, 515−560 nm excitation, 590 long pass emission; Molecular Probes) at 37 °C as previously described.[8] Fluorescent signal was measured on a Hamamatsu Orca ER digital camera attached to an inverted Nikon TE2000-U microscope. An equivalent region not containing cells was used as background and was subtracted. Fluorescent images were taken at 1 min intervals with an exposure of 200 ms. Ratio of fluorescence was reported as the slope of the signal measured at 22−40 min (treatment) over the slope of the signal measured at 0−20 min (basal). DHE fluorescence was stimulated by the addition of BayK(−) (10 μM). Nisoldipine (20 μM) was used to verify increases in DHE fluorescence were a result of BayK(−) stimulation. Metamorph 6.3 was used to quantify the signal by manually tracing myocytes.

In Vitro Drug Release Studies. 6 mg of each of resveratrol and curcumin loaded nanoparticles were dispersed in 12 mL of PBS (pH 7.4) with 0.2% w/v Tween 80 as a sink to monitor release kinetics. The suspension was divided in 24 vials of 500 μL (0.25 mg NP) each. Samples were then put into an orbital shaker at 125 rpm, 37 °C. At given time intervals, samples were taken out in triplicates and centrifuged at 16000*g* for 30 min. The supernatant was extracted and analyzed for curcumin and resveratrol. In the case of curcumin nanoparticles, the supernatant was analyzed for released curcumin content using UV−vis absorption at 425 nm. These values were compared with a standard curve of absorption *versus* concentration for curcumin dissolved in the release medium as used at 425 nm (see Figure S2). In the case of resveratrol nanoparticles, due to the lower loading the release profile was calculated by monitoring the drug loading over time.

In this case the pellet (0.25 mg) was redispersed in 500 μL of methanol and sonicated in a water bath for 10 min followed by an hour of incubation to extract out unreleased drug. Samples were then centrifuged at 16000*g* for 20 min to separate polymeric nanoparticles. Drug containing methanol samples were analyzed for resveratrol content using UV−vis absorption at 323 nm. These values were compared with standard curve of resveratrol in methanol at 323 nm generated previously (see Figure S3).

Statistical Analysis. All cardiac assay data are presented as mean ± standard error of the mean (SEM). Standard deviation was used in some analyses. Statistical comparisons between multiple groups were made using one-way ANOVA, with Tukey's test applied post hoc to compare unpaired means. *P*-values <0.05 were considered significant (GraphPad Prism 6.0).

Conflict of Interest: The authors declare no competing financial interest.

Acknowledgment. The authors would like to acknowledge Prof. Igor Luzinov and Dr. Bogdan Zydyrko from the School of Materials Science and Engineering, Clemson University, Clemson, SC, USA for the synthesis of the poly(glycidyl methacrylate) used to synthesis the polymeric nanoparticles. The authors acknowledge assistance from the Australian Microscopy & Microanalysis Research Facility at the Centre for Microscopy, Characterisation & Analysis, The University of Western Australia. This work was funded by the Australian Research Council (ARC), and the National Health & Medical Research Council (NHMRC) of Australia. Helena Viola is a Heart Foundation of Australia Postdoctoral Research Fellow, K. Swaminathan Iyer is an ARC Future Fellow and Livia Hool is an ARC Future Fellow and Honorary NHMRC Senior Research Fellow.

Supporting Information Available: Contains dynamic light scattering and zeta potential measurements of the curcumin-loaded and the resveratrol-loaded multifunctional PGMA nanoparticles and release profiles. This material is available free of charge *via* the Internet at http://pubs.acs.org.

REFERENCES AND NOTES

1. Yellon, D. M.; Hausenloy, D. J. Mechanisms of Disease: Myocardial Reperfusion Injury. *New Engl. J. Med.* **2007**, *357*, 1121–1135.
2. Opie, L. H. Reperfusion Injury and Its Pharmacologic Modification. *Circulation* **1989**, *80*, 1049–1062.
3. Frey, N.; Olson, E. N. Cardiac Hypertrophy: The Good, the Bad, and the Ugly. *Annu. Rev. Physiol.* **2003**, *65*, 45–79.
4. Bodi, I.; Muth, J. N.; Hahn, H. S.; Petrashevskaya, N. N.; Rubio, M.; Koch, S. E.; Varadi, G.; Schwartz, A. Electrical Remodeling in Hearts from a Calcium-Dependent Mouse Model of Hypertrophy and Failurecomplex Nature of K^+ Current Changes and Action Potential Duration. *J. Am. Coll. Cardiol.* **2003**, *41*, 1611–1622.
5. Seddon, M.; Looi, Y. H.; Shah, A. M. Oxidative Stress and Redox Signalling in Cardiac Hypertrophy and Heart Failure. *Heart* **2007**, *93*, 903–907.
6. Pragnell, M.; De Waard, M.; Mori, Y.; Tanabe, T.; Snutch, T. P.; Campbell, K. P. Calcium Channel Beta-Subunit Binds to a Conserved Motif in the I-II Cytoplasmic Linker of the Alpha 1-Subunit. *Nature* **1994**, *368*, 67–70.
7. Viola, H. M.; Hool, L. C. Cross-Talk between L-Type Ca^{2+} Channels and Mitochondria. *Clin. Exp. Pharmacol. Physiol.* **2010**, *37*, 229–235.
8. Viola, H. M.; Arthur, P. G.; Hool, L. C. Transient Exposure to Hydrogen Peroxide Causes an Increase in Mitochondria-Derived Superoxide as a Result of Sustained Alteration in L-Type Ca^{2+} Channel Function in the Absence of Apoptosis in Ventricular Myocytes. *Circ. Res.* **2007**, *100*, 1036–1044.
9. Venardos, K. M.; Kaye, D. M. Myocardial Ischemia-Reperfusion Injury, Antioxidant Enzyme Systems, and Selenium: A Review. *Curr. Med. Chem.* **2007**, *14*, 1539–1549.
10. Tang, H.; Viola, H. M.; Filipovska, A.; Hool, L. C. $Ca_v1.2$ Calcium Channel Is Glutathionylated During Oxidative Stress in Guinea Pig and Ischemic Human Heart. *Free Radical Biol. Med.* **2011**, *51*, 1501–1511.
11. Eltzschig, H. K.; Eckle, T. Ischemia and Reperfusion—from Mechanism to Translation. *Nat. Med.* **2011**, *17*, 1391–1401.
12. Frey, N.; Katus, H. A.; Olson, E. N.; Hill, J. A. Hypertrophy of the Heart: A New Therapeutic Target? *Circulation* **2004**, *109*, 1580–1589.
13. Li, Y.; Ha, T.; Gao, X.; Kelley, J.; Williams, D. L.; Browder, I. W.; Kao, R. L.; Li, C. NF-kappaB Activation Is Required for the Development of Cardiac Hypertrophy *in Vivo*. *Am. J. Physiol.: Heart Circ. Physiol.* **2004**, *287*, H1712–20.
14. Zorov, D. B.; Filburn, C. R.; Klotz, L.-O.; Zweier, J. L.; Sollott, S. J. Reactive Oxygen Species (ROS-Induced) ROS Release a New Phenomenon Accompanying Induction of the Mitochondrial Permeability Transition in Cardiac Myocytes. *J. Exp. Med.* **2000**, *192*, 1001–1014.
15. Aon, M. A.; Cortassa, S.; Marbán, E.; O'Rourke, B. Synchronized Whole Cell Oscillations in Mitochondrial Metabolism Triggered by a Local Release of Reactive Oxygen Species in Cardiac Myocytes. *J. Biol. Chem.* **2003**, *278*, 44735–44744.
16. Seenarain, V.; Viola, H. M.; Ravenscroft, G.; Casey, T. M.; Lipscombe, R. J.; Ingley, E.; Laing, N. G.; Bringans, S. D.; Hool, L. C. Evidence of Altered Guinea Pig Ventricular Cardiomyocyte Protein Expression and Growth in Response to a 5 min *in Vitro* Exposure to H_2O_2. *J. Proteome Res.* **2010**, *9*, 1985–1994.
17. Viola, H. M.; Hool, L. C. Role of the Cytoskeleton in Communication between L-Type Ca^{2+} Channels and Mitochondria. *Clin. Exp. Pharmacol. Physiol.* **2013**, *40*, 295–304.
18. Viola, H. M.; Arthur, P. G.; Hool, L. C. Evidence for Regulation of Mitochondrial Function by the L-Type Ca2+ Channel in Ventricular Myocytes. *J. Mol. Cell. Cardiol.* **2009**, *46*, 1016–1026.
19. Viola, H.; Adams, A. M.; Davies, S. M. K.; Fletcher, S.; Filipovska, A.; Hool, L. C. Impaired Functional Communication between the L-Type Calcium Channel and Mitochondria Contributes to Metabolic Inhibition in the mdx Heart. *Proc. Natl. Acad. Sci. U. S. A.* **2014**, *111*, 2905–2914.
20. Clemons, T. D.; Viola, H. M.; House, M. J.; Iyer, K. S.; Hool, L. C. Examining Efficacy of "TAT-Less" Delivery of a Peptide against the L-Type Calcium Channel in Cardiac Ischemia-Reperfusion Injury. *ACS Nano* **2013**, *7*, 2212–20.
21. Viola, H. M.; J, M.; Roos, K. P.; Hool, L. C. Decreased Myocardial Injury and Improved Contractility after Administration of a Peptide Derived against the Alpha-Interacting Domain of the L-Type Calcium Channel. *J. Am. Heart Assoc.* **2014**, 10.1161/JAHA.114.000961.
22. Viola, H. M.; Hool, L. C. How Does Calcium Regulate Mitochondrial Energetics in the Heart?—New Insights. *Heart, Lung Circ.* **2014**, *23*, 602.
23. Hohaus, A.; Poteser, M.; Romanin, C.; Klugbauer, N.; Hofmann, F.; Morano, I.; Haase, H.; Groschner, K. Modulation of the Smooth-Muscle L-Type Ca^{2+} Channel Alpha1 Subunit (Alpha1c-B) by the Beta2a Subunit: A Peptide Which Inhibits Binding of Beta to the I-II Linker of Alpha1 Induces Functional Uncoupling. *Biochem. J.* **2000**, *348* (Pt 3), 657–665.
24. Viola, H. M.; J, M.; Roos, K. P.; Hool, L. C. Decreased Myocardial Injury and Improved Contractility after Administration of a Peptide Derived against the Alpha-Interacting Domain of the L-Type Calcium Channel. *J. Am. Heart Assoc.* **2014**, *23*, e000961.
25. Wongcharoen, W.; Phrommintikul, A. The Protective Role of Curcumin in Cardiovascular Diseases. *Int. J. Cardiol* **2009**, *133*, 145–151.
26. Chen, J.; Chow, S. Antioxidants and Myocardial Ischemia: Reperfusion Injuries. *Chang Gung Med. J.* **2005**, *28*, 369.
27. Kim, Y. S.; Kwon, J. S.; Cho, Y. K.; Jeong, M. H.; Cho, J. G.; Park, J. C.; Kang, J. C.; Ahn, Y. Curcumin Reduces the Cardiac Ischemia-Reperfusion Injury: Involvement of the Toll-Like Receptor 2 in Cardiomyocytes. *J. Nutr. Biochem.* **2012**, *23*, 1514–1523.
28. Fiorillo, C.; Becatti, M.; Pensalfini, A.; Cecchi, C.; Lanzilao, L.; Donzelli, G.; Nassi, N.; Giannini, L.; Borchi, E.; Nassi, P. Curcumin Protects Cardiac Cells against Ischemia-Reperfusion Injury: Effects on Oxidative Stress, Nf-Kappa B, and Jnk Pathways. *Free Radical Biol. Med.* **2008**, *45*, 839–846.

29. Anitha, A.; Deepagan, V. G.; Divya Rani, V. V.; Menon, D.; Nair, S. V.; Jayakumar, R. Preparation, Characterization, *in Vitro* Drug Release and Biological Studies of Curcumin Loaded Dextran Sulphate−Chitosan Nanoparticles. *Carbohydr. Polym.* **2011**, *84*, 1158–1164.
30. Santos, A. C.; Veiga, F.; Ribeiro, A. J. New Delivery Systems to Improve the Bioavailability of Resveratrol. *Expert Opin. Drug Delivery* **2011**, *8*, 973–990.
31. Anand, P.; Nair, H. B.; Sung, B.; Kunnumakkara, A. B.; Yadav, V. R.; Tekmal, R. R.; Aggarwal, B. B. Design of Curcumin-Loaded PLGA Nanoparticles Formulation with Enhanced Cellular Uptake, and Increased Bioactivity *in Vitro* and Superior Bioavailability *in Vivo*. *Biochem. Pharmacol.* **2010**, *79*, 330–338.
32. Amri, A.; Chaumeil, J. C.; Sfar, S.; Charrueau, C. Administration of Resveratrol: What Formulation Solutions to Bioavailability Limitations? *J. Controlled Release* **2012**, *158*, 182–193.
33. Nair, K. L.; Thulasidasan, A. K. T.; Deepa, G.; Anto, R. J.; Kumar, G. S. V. Purely Aqueous Plga Nanoparticulate Formulations of Curcumin Exhibit Enhanced Anticancer Activity with Dependence on the Combination of the Carrier. *Int. J. Pharm.* **2012**, *425*, 44–52.
34. Zweier, J. L.; Talukder, M. A. The Role of Oxidants and Free Radicals in Reperfusion Injury. *Cardiovasc. Res.* **2006**, *70*, 181–190.
35. Becker, L. B. New Concepts in Reactive Oxygen Species and Cardiovascular Reperfusion Physiology. *Cardiovasc. Res.* **2004**, *61*, 461–470.
36. Sun, S.; Zeng, H.; Robinson, D. B.; Raoux, S.; Rice, P. M.; Wang, S. X.; Li, G. Monodisperse MFe_2O_4 (M= Fe, Co, Mn) Nanoparticles. *J. Am. Chem. Soc.* **2004**, *126*, 273–279.
37. Evans, C. W.; Fitzgerald, M.; Clemons, T. D.; House, M. J.; Padman, B. S.; Shaw, J. A.; Saunders, M.; Harvey, A. R.; Zdyrko, B.; Luzinov, I.; Silva, G. A.; Dunlop, S. A.; Iyer, K. S. Multimodal Analysis of Pei-Mediated Endocytosis of Nanoparticles in Neural Cells. *ACS Nano* **2011**, *5*, 8640–8648.
38. Dandekar, P. P.; Patravale, V. B. Development and Validation of a Stability-Indicating LC Method for Curcumin. *Chromatographia* **2009**, *69*, 871–877.
39. Ansari, K. A.; Vavia, P. R.; Trotta, F.; Cavalli, R. Cyclodextrin-Based Nanosponges for Delivery of Resveratrol: *in Vitro* Characterisation, Stability, Cytotoxicity and Permeation Study. *AAPS PharmSciTech* **2011**, *12*, 279–286.
40. Dinkova-Kostova, A. T.; Talalay, P. Relation of Structure of Curcumin Analogs to Their Potencies as Inducers of Phase 2 Detoxification Enzymes. *Carcinogenesis* **1999**, *20*, 911.
41. Rahman, I.; Kode, A.; Biswas, S. K. Assay for Quantitative Determination of Glutathione and Glutathione Disulfide Levels Using Enzymatic Recycling Method. *Nat. Protoc.* **2006**, *1*, 3159–3165.
42. Viola, H. M.; Davies, S. M.; Filipovska, A.; Hool, L. C. L-Type Ca^{2+} Channel Contributes to Alterations in Mitochondrial Calcium Handling in the mdx Ventricular Myocyte. *Am. J. Physiol.: Heart Circ. Physiol.* **2013**, *304*, H767–775.